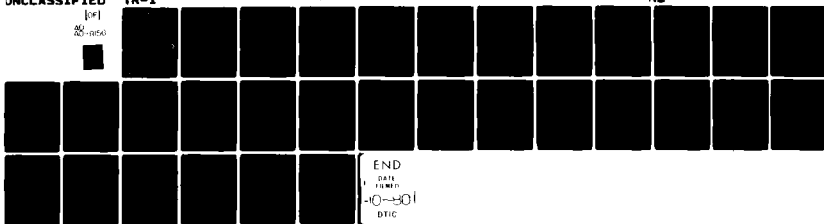


AD-A089 156

NORTHWESTERN UNIV EVANSTON IL DEPT OF CHEMISTRY F/6 7/4
IMAGE FIELD THEORY OF ENHANCED RAMAN SCATTERING BY MOLECULES AB--ETC(U)
SEP 80 G C SCHATZ, R P VAN DUYN N00014-79-C-0794
UNCLASSIFIED TR-1 NL

[*]
88-056



END
DATA
FORM
10-80
DTC

AD A089156

LEVEL

12

OFFICE OF NAVAL RESEARCH

Contract N00014-79-C-0794

TECHNICAL REPORT No. 1

Image Field Theory of Enhanced Raman Scattering by Molecules Adsorbed
on Metal Surfaces: Detailed Comparison with Experimental Results

by

G. C. Schatz and R. P. Van Duyne

Prepared for Publication

in

Surface Science

Department of Chemistry
Northwestern University
Evanston, Illinois 60201

September 1980

Reproduction in whole or in part is permitted for any
purpose of the United States Government

This document has been approved for public release and sale;
its distribution is unlimited

DTIC
ELECTE
SEP 17 1980

DDC FILE COPY

80 9 15 023

REPORT DOCUMENTATION PAGE		READ INSTRUCTIONS BEFORE COMPLETING FORM
1. REPORT NUMBER	2. GOVT ACCESSION NO.	3. RECIPIENT'S CATALOG NUMBER
	AD-A089156	
4. TITLE (and Subtitle)	5. TYPE OF REPORT & PERIOD COVERED	
Image Field Theory of Enhanced Raman Scattering by Molecules Adsorbed on Metal Surfaces: Detailed Comparison with Experimental Results.	Technical Report.	
7. AUTHOR(s)	6. PERFORMING ORG. REPORT NUMBER	
George Schatz and R. P. Van Duyne		
9. PERFORMING ORGANIZATION NAME AND ADDRESS	8. CONTRACT OR GRANT NUMBER(s)	
Department of Chemistry Northwestern University Evanston, Illinois 60201	N00014-79-C-0794	
11. CONTROLLING OFFICE NAME AND ADDRESS	10. PROGRAM ELEMENT, PROJECT, TASK AREA & WORK UNIT NUMBERS	
Office of Naval Research Department of the Navy Arlington, VA. 22217	1715 Set 8	
14. MONITORING AGENCY NAME & ADDRESS (if different from Controlling Office)	12. REPORT DATE	
12/32/	September 15, 1980	
	13. NUMBER OF PAGES	
	29	
	15. SECURITY CLASS. (of this report)	
	Unclassified	
	15a. DECLASSIFICATION/DOWNGRADING SCHEDULE	
16. DISTRIBUTION STATEMENT (of this Report)		
Approved for public release and sale; distribution unlimited		
17. DISTRIBUTION STATEMENT (of the abstract entered in Block 20, if different from Report)		
18. SUPPLEMENTARY NOTES		
19. KEY WORDS (Continue on reverse side if necessary and identify by block number)		
Surface Enhanced Raman Spectroscopy(SERS), Image Field Model, Spectroscopic studies of molecular adsorption on metals		
20. ABSTRACT (Continue on reverse side if necessary and identify by block number)		
An image field theory of surface enhanced Raman spectroscopy is used to study the dependence of Raman intensities on light frequency, nature of adsorbate and metal, electrode potential, scattering angle and light polarization. Although the image field enhancement (IFE) theory is at best a crude approximation to the true enhancement mechanism, we do find quite reasonable agreement between the IFE predictions and most existing experimental results.		

26080

JOB

IMAGE FIELD THEORY OF ENHANCED RAMAN SCATTERING BY
MOLECULES ADSORBED ON METAL SURFACES: DETAILED
COMPARISON WITH EXPERIMENTAL RESULTS

GEORGE C. SCHATZ and RICHARD P. VAN DUYNE

Department of Chemistry, Northwestern University,

Evanston, IL 60201 USA

Received

An image field theory of surface enhanced Raman spectroscopy is used to study the dependence of Raman intensities on light frequency, nature of the adsorbate and metal, electrode potential, scattering angle and light polarization. Although the image field enhancement (IFE) theory is at best a crude approximation to the true enhancement mechanism, we do find quite reasonable agreement between the IFE predictions and most existing experimental results.

Accession For	
NTIS GRA&I	<input checked="" type="checkbox"/>
DDC TAB	<input type="checkbox"/>
Unannounced Justification	<input type="checkbox"/>
By _____	
Distribution/	
Availability CODE	
Dist	Available for special
A	

1. Introduction

One of the most important discoveries in the field of surface science in the last few years is the observation [1, 2] of enormously enhanced cross sections (factors of 10^6) for Raman scattering from molecules adsorbed on metal surfaces. (See Ref. 3 for a review of recent literature.) This so-called Surface Enhanced Raman Spectroscopy (SERS) enables the determination of detailed structural information about adsorbed molecules even in submonolayer coverages, and in both solid-gas and solid-liquid environments. Although SERS has been the subject of intense study, its interpretation is still a subject of much controversy, with at least six mechanisms (not all independent) proposed. These include: (1) image field enhancement (IFE) of the adsorbate polarizability [4, 5], (2) polarizability enhancement by strong static fields present in the interfacial environment [2b, 6], (3) resonant or preresonant enhancement arising from coupling of electron hole pair excited states in the metal to the adsorbate vibrations [7], (4) resonant enhancement caused by coupling of the molecular electronic states to surface plasmon states [8], (5) Raman scattering in reflectance from the metal arising from modulation of the surface dielectric constant by the vibrating adsorbate charge distribution [9], and (6) resonant Raman enhancement arising from the presence of metal-adsorbate charge transfer states [10]. While all of these mechanisms can at least qualitatively explain some features of the SERS experimental data (mainly the enhancement effect itself), there exists a growing body of data concerning the frequency,

polarization, angular, metal, adsorbate, and electrode potential dependence of SERS which should make it possible to distinguish (and eliminate) some of these mechanisms in the near future.

In this paper, we examine the IFE mechanism in detail, making comparisons of its predictions with recent experimental results, in an attempt to assess its reliability. We will not simultaneously test the other mechanisms, mainly because only the IFE mechanism has been developed sufficiently to enable quantitative predictions about most experimental observables. We do, however, suggest that the comparisons made here also be considered in future studies of other mechanisms.

2. Theoretical Description of SERS Using the IFE Mechanism

The IFE mechanism was originally proposed by King, Van Duyne, and Schatz [4] and has also been extensively studied by Efrima and Metiu [5]. In it, one assumes (see Fig. 1) that an incident light beam of frequency ν at an angle θ_i scatters off molecules (with dielectric constant ϵ_A) adsorbed on the surface of a metal (with dielectric constant ϵ_M) to an outgoing beam of frequency ν' at an angle θ_o . The Raman intensity is calculated using the usual classical theory of light scattering, but in doing so, we include for the fact that geometrical and image effects modify the scattering in several ways relative to scattering in the absence of the surface [4, 5]. The geometrical effects include the effect of superposition of the direct and reflected incident and scattered waves (paths 1-2 and 3-4 in Fig. 1), and the effect of incomplete orientation averaging due to hindered rotational

motions of the adsorbate. If the metal were a perfect mirror (i. e., $\text{Re } \epsilon_M \rightarrow -\infty$), and the adsorbate were close to the surface ($R \rightarrow 0$), the superposition effect would lead to cancellation of all but the components of the incident and outgoing electric fields perpendicular to the surface. This implies that only p-polarized scattering would occur (polarized parallel to the plane of incidence), but for any real metal, the intensity of s-polarized scattering is also nonzero, as is determined by the Fresnel reflection coefficients. Since these coefficients are functions of θ_i , θ_o , ϵ_M , and ϵ_A [11], they influence some aspects of the angular, metal, adsorbate, frequency and electrode potential dependence of the scattered intensity. Their contribution to the enhancement in scattered intensity is usually relatively small [4, 5].

The largest intensity changes in this model arise from the influence of the image field effect on the adsorbate polarizability. As is described more thoroughly in Ref. 4, the electric field \tilde{E} of the electromagnetic wave induces an oscillating dipole $\tilde{\mu}_{\text{ind}}$ in the adsorbate, which in turn induces an image dipole $\tilde{\mu}_{\text{image}}$ in the metal. $\tilde{\mu}_{\text{image}}$ has a field \tilde{E}_{image} associated with it, which adds constructively to \tilde{E} , and enhances the overall field experienced by the molecule. This makes $\tilde{\mu}_{\text{ind}}$ larger and since the apparent adsorbate polarizability α_A is proportional to $\tilde{\mu}_{\text{ind}}$, this is also larger. If we replace the molecule by a point dipole located at a distance R from the surface (admittedly a crude assumption) and also assume that the polarizability tensor is diagonal in the coordinate system

xyz depicted in Fig. 1, we find [4] that the zz element of $\alpha_{\approx A}$ is given by

$$\alpha_{A_{zz}} = \alpha_{zz} (1 - \gamma \alpha_{zz}/4R^3)^{-1} \quad (1)$$

where α_{zz} is the corresponding element of the molecular polarizability tensor in the absence of the metal, and $\gamma = (\epsilon_M - \epsilon_A)/(\epsilon_M + \epsilon_A)\epsilon_A$. The factor in parentheses in Eq. (1) is an enhancement factor which will play an important role in the IFE mechanism. Although this result was derived using an image field approximation to the solution of Maxwell's equations, a more detailed analysis [5] shows that for the small R/λ values characteristic of most experiments (where λ is the wavelength of incident light), Eq. (1) is accurate to within a few per cent of the exact solution.

The scattered intensity I_A actually depends on the derivative of the polarizability with respect to the vibrational normal coordinate Q for the Raman transition of interest, and from Eq. (1), we find

$$\frac{d\alpha_{A_{zz}}}{dQ} = \frac{d\alpha_{zz}}{dQ} (1 - \gamma \alpha_{zz}/4R^3)^{-2} \quad (2)$$

The general expression relating $d\alpha_{A_{zz}}/dQ$ to I_A depends on the polarization of the incident and outgoing waves (s or p), and is given in Ref. 5b. Here we write down the expression for the special case of p-polarized incident and scattered waves, and an α_{\approx} tensor having only α_{zz} nonzero:

$$I_A = I_0 \frac{\omega'^4}{c^4} |1 + R_p^i|^2 |1 + R_p^o|^2 \sin^2 \theta_i \sin^2 \theta_o \left| \frac{d\alpha_{ZZ}}{dQ} \right|^2 |Q^2| \quad (3)$$

Here I_0 is the incident light intensity, $\omega' = 2\pi\nu'$, R_p^i and R_p^o are the Fresnel reflection coefficients for p-polarized light [11], and $|Q^2|$ is the mean square normal coordinate displacement. Substituting Eq. (2) into Eq. (3) and taking the ratio of the resulting I_A (evaluated at θ_i, θ_o for which I_A maximizes) to the corresponding orientation averaged solution intensity (evaluated at the scattering angle for which it maximizes) leads to the following expression for the intensity enhancement:

$$e = \left\{ \frac{15}{8} |1 + R_p^i|^2 |1 + R_p^o|^2 \sin^2 \theta_i \sin^2 \theta_o \right\} \left| 1 - \frac{\gamma \alpha_{ZZ}}{4R^3} \right|^{-4} \quad (4)$$

The expression in braces in (4) represents the contribution of geometrical factors to the enhancement, and could be defined in other ways. It does not, however, play an important role in the intensity enhancement (maximum value is 30). The $|1 - \gamma \alpha_{ZZ} / 4R^3|^{-4}$ factor can be much more important, and in Section III. B, we will attempt to estimate its magnitude for comparison with experiment.

III. Theoretical Predictions, Experimental Comparisons

III. A Angular Distributions, Depolarization Ratios, Selection Rules

Although the prefactors $|1 + R_p^i|^2 |1 + R_p^o|^2 \sin^2 \theta_i \sin^2 \theta_o$ in Eq. (3) play only a minor role in determining Raman intensities, they are

solely responsible for the angular dependence of Raman scattering. In addition, the geometrical factors discussed above which are responsible for these prefactors also determine the depolarization ratios and selection rules. This is of particular significance because these same prefactors also appear in some of the other postulated mechanisms of the SERS effect, which means that comparisons of the angular, polarization and selection information which they control does not uniquely test the intensity enhancement mechanism. It is nevertheless useful to examine the predictions of these prefactors, since they do test the validity of the geometrical aspects of the model in Fig. 1.

The dependence of I_A on θ_i or θ_o obtained from Eq. (3) is plotted in Fig. 2 (using ϵ_M appropriate for Ag [12] at 5490 Å and $\epsilon_A = 1.76$). The analogous s-polarized intensity is also shown, and it is seen to be quite small even for this non-perfect mirror case. The p-polarized intensity is seen to maximize near $\theta_i = \theta_o = 60^\circ$, which is a conclusion similar to one reached by Greenler and Slager [13] for a similar model well before the SERS effect was discovered. Experimentally, the only measured SERS angular distribution is the very recent result of Pettinger, Wenning and Wetzl [14a] for pyridine on Ag. This very surprisingly shows sharp peaks in the angular dependence, rather than a broad distribution such as might be expected from Fig. 2. (Their instrumental geometry was such that θ_o was constrained to equal $\pi/2 - \theta_i$, so the IFE angular dependence for their case is predicted to peak at 45° .) Of course, their result could be due to a coherent superposition of the emitted fields of all the adsorbed molecules

(assuming that this overlayer is ordered). This would be consistent with the observed broadening of the angular distribution when the surface is deliberately roughened.

All of the determinations of the depolarization ratios have been on rough surfaces, and for geometries which tend to obscure the differences between s and p polarized intensities indicated in Fig. 2 [2a, 9a]. For a geometry which simulates that used by Jeanmaire and Van Duyne [2a], one can make a crude estimate of the IFE depolarization ratio by angle averaging to mimic the effects of roughness. This gives depolarization ratios in the 0.5-1.0 range, which compares favorably with the value 0.57 which they measured for pyridine.

A more detailed comparison with experiment is provided by considering selection rules, the simplest of which states that the intensity is zero if $d\alpha_{zz}/dQ$ is zero. This is a consequence of Eqs. (2) and (3) (although it is consistent with some of the other mechanisms as well [8b, 14b]) and holds strictly even when none of the polarizability tensor elements are zero if the metal is a perfect mirror. For nonperfect mirrors, elements of the polarizability tensor other than $d\alpha_{zz}/dQ$ appear in the intensity expression and the selection rule is partially relaxed. Despite this, there is reasonably good agreement between the predictions of the selection rule and experimental results for pyridine, and 2,3,4-cyanopyridines on silver [2, 3, 15]. In pyridine for example, spectral features corresponding to the a_2 (out of plane bending) mode are either weak or absent in the observed spectra

although features corresponding to all the other modes are much stronger (with the zz polarized irreducible representation dominant). For 2,3,4-cyanopyridines, the CN stretch intensity was found to be proportional to the square of the projection of the normal coordinate displacement on the z axis, which is also consistent with $I_A \propto |d\alpha_{zz}/dQ|^2$. We should caution here that in all of these experiments, the adsorption geometry is still the subject of significant uncertainty, and this makes the definitive testing of selection rules difficult.

III. B Frequency, Metal, Adsorbate and Electrode Potential Dependence of Intensity Enhancements

To use the IFE theory to predict Raman intensity enhancements, including the dependence on light frequency, nature of metal and adsorbate, and electrode potential, requires only the substitution of ϵ_M , ϵ_A , α_{zz} and R into Eq. (4). Although there is some uncertainty concerning what are the best choices for all of these parameters in this evaluation, ϵ_M , ϵ_A and α_{zz} can be reasonably estimated using the bulk or gas phase values. The parameter R is however very uncertain, not only because the geometry of the adsorbate-metal complex is unknown, but also because the location of the point dipole μ_{ind} relative to an image plane is not well defined. Although there has been much discussion and computation concerning best choices for locating static dipoles for image theory treatments [16], the analogous treatment of oscillating dipoles has not been considered, and the best "prescription" for assigning R remains uncertain. This is a major problem

with the image field mechanism, for the R dependence of ϵ can be quite strong. If we consider pyridine on Ag, using literature values of ϵ_M at 5214 Å [12], α_{ZZ} [5], and a value of ϵ_A equal to that of water (1.76), we obtain the ϵ versus R curve plotted in Fig. 3 (labelled $\sigma = 0$). At $R = 1.41$ Å, Fig. 3 shows an enhancement of over 10^7 , but the curve is highly peaked, and a "reasonable" value of R (obtained by summing covalent radii and applying various corrections [4]) is probably closer to 1.6-1.7 Å, where $\epsilon \approx 10^2$ - 10^3 . Efrima and Metiu have noted [5c] that if a two state expression for the adsorbate polarizability α_{ZZ} is used in Eq. (1), the resulting expression for $\alpha_{A,ZZ}$ has the form of a two state polarizability wherein the frequency ω_0 of the upper state is shifted downwards to $\omega_0 = \omega_e (1 - \alpha_{ZZ}(0) \text{Re } \gamma / 4R^3)^{1/2}$ (where ω_e is excited state energy in the absence of the surface and $\alpha_{ZZ}(0)$ is the zero frequency polarizability), and its width increased by $\alpha_{ZZ}(0) \omega_e^2 \text{Im } \gamma / 8R^3 \omega_0$. An analogous shifting also occurs when many state polarizability expansions are used as in the present case. One can then show that the sharp peak at $R = 1.41$ Å in Fig. 3 occurs when the energy of the lowest excited state is shifted into resonance with the photon energy. To the extent that the many state expansion of the polarizability is an adequate representation of α_{ZZ} , one can consider that the large enhancement in ϵ results from this surface induced resonant effect, and this is the point of view of Ref. 5c. While this may be an oversimplification, the qualitative behavior of ϵ for $R > 1.5$ Å would probably not change drastically if other representations of α_{ZZ} were used.

Efrima and Metiu have also noted [5c] that a more

realistic estimate of ϵ can be obtained by averaging Eq. (4) over a distribution of R (to simulate a distribution of possible distances from the surface). Using a Gaussian distribution with rms deviation $\sigma = 0.1 \text{ \AA}$ yields the curve with that label in Fig. 3. This shows much less sensitivity of ϵ to R , although it is clear that ϵ continues to fall off rapidly with increasing R for $R > 1.7 \text{ \AA}$. The enhancement estimate for $R = 1.6 - 1.7 \text{ \AA}$ is now $\sim 10^5$ which is much closer to the experimental estimate [3] of 10^6 . In addition, the requirement of proximity to the surface agrees with the conclusions of recent UHV experiments by Smardzewski *et al.* [17]. Realistically, however, all that we can legitimately conclude from this analysis is that an enhancement by several orders of magnitude is possible with the IFE mechanism for molecules suitably close to the surface. We can also state that there appears to be nothing special about pyridine in this treatment, for there are many molecules with similar polarizabilities and adsorption distances. This would explain why this effect has been observed for such an abundance of molecules adsorbed on silver [2, 3]. This generality with respect to adsorbates should also apply to resonance Raman scatterers, and this would appear to explain why the effect has been seen using dye molecules on Ag [2a] with the combination of both surface and resonant enhancement responsible for a 10^{10} increase in intensity over normal Raman solution cross sections.

To study the frequency dependence of the enhancement, we arbitrarily choose R such that the position averaged ϵ matches experiment

at some frequency (say $R = 1.6 \text{ \AA}$ and $\hbar\omega = 2.38 \text{ eV}$ so that $\epsilon = 5 \times 10^5$ in Fig. 3), then use that R to determine ϵ at other frequencies. The resulting frequency dependence is compared with experiment [3] in Fig. 4. The theoretical curve, which matches well one previously given by Efrima and Metiu [5c] shows a largely flat dependence (i. e., ω^4 scattering) for $\hbar\omega < 2.6 \text{ eV}$, then a rapid fall off for larger $\hbar\omega$, with intensity going to nearly zero at the surface plasmon frequency (3.6 eV). Experimental results are available only over the relatively restricted frequency range 1.9-2.7 eV, plus a few isolated measurements in the 3.4-4.4 eV range. The experiments show somewhat different frequency dependences for different modes, with the 1008 cm^{-1} ring breathing mode showing a gradual decrease in ϵ with increasing $\hbar\omega$ between 1.9 and 2.7 eV, and the 1215 cm^{-1} mode showing a nearly flat dependence in that range. For both modes, the change in ϵ over the 1.9-2.7 eV range is small, so the agreement with the relatively flat IFE result is not unreasonable. Presumably the effect of different vibrational modes might be modelled by choosing a mode dependent R value. Although no criterion exists for choosing this R at present, we do find that the use of different R 's in Eq. (4) leads to slightly different frequency dependences in the 1.9-2.7 eV range, including the possibility of a decreasing ϵ with increasing $\hbar\omega$ similar to the 1008 cm^{-1} result. The sharp drop-off in enhancement near 3 eV is relatively insensitive to the choice of R , and arises because the opening of the surface plasmon excitation channel destroys the high reflectivity

properties of Ag, thereby reducing the image effect. Experimentally, since no signals are detected at all in the 3.4-4.4 eV range, only upper bounds to the enhancements can be reported. A simple estimate of detection sensitivity indicates [3] that for the apparatus used for these measurements (described in Refs. 2,3) an enhancement of roughly 10^3 is needed to observe any signal, and we have used this estimate as the upper bound in Fig. 4.

The predicted dependence of enhancement on the nature of the metal substrate can be estimated by assuming that only ϵ_M in Eq. (4) changes in going from one metal to another. This of course ignores differences in adsorption characteristics, but does provide some indication for the intrinsic ability of other metals to exhibit the image effect. Among other metals that have been investigated are Au, Cu, and Pt, and in Fig. 5 we use ϵ_M values from Refs. 11, 18, and 19 to estimate the predicted enhancements for Raman scattering from these metals, comparing the results with that for Ag. It is immediately apparent that at the experimentally accessible frequency of 2.5 eV, Au, Pt and Cu all have relatively low enhancements, and this may explain the rather poor spectra which have been obtained in experiments with these metals [20]. Both Au and Cu are predicted to be significantly more favorable for $\hbar\omega \ll 2.0$ eV, and this appears to correlate well with recent observations (See Fig.5) of well resolved SERS spectra for molecules on these metals near 1.9eV[21]. A surprisingly intense spectrum of I_2 on Au at 2.4 eV has also been recently observed [22], however the I_2 in this case is resonantly enhanced and this may be responsible for the enhancement

observed. Obviously what is needed at this point is a systematic study of the frequency dependence of the Raman intensities for the I_2/Au and I_2/Ag systems to disentangle resonance from surface enhancement effects. It is interesting to note that although most transition metals show strong interband transitions in the visible region which make them poor candidates for SERS applications, many of these same metals become much more favorable in the near IR. In addition, there are some nontransition metals which seem to have favorable enough dielectric properties to enable SERS experiments in the visible, including Al and the alkali metals. Obviously it would be highly desirable to test these IFE predictions experimentally, for the extension of SERS to metals other than Ag would be very useful.

The variation of intensity with changes in electrode potential can also be described by the image field mechanism, although in this case three competing effects are possible, and the relative importance of each has yet to be determined. First, the concentration of surface adsorbed species is known to be a strong function of electrode potential, with peak concentrations obtained near the point of zero charge of the metal for adsorbed neutral organic molecules [23]. Second, surface polarization effects can cause the metal dielectric constant to vary as a function of electrode potential in the Thomas-Fermi layer (typically the top 0.5 Å of the metal). This is responsible for the related phenomenon of electroreflectance [24], and could lead to a dependence of ϵ on electrode potential. Third, gas phase experiments have shown [25], that frequency dependent

polarizabilities can be functions of static electric field strengths in the presence of strong fields such as are present in the interfacial region. These fields are, of course, changed by varying the electrode potential, which implies that the enhancement could also change. The combination of these three factors will typically lead to intensities that show a peak near the point of zero charge as a function of electrode potential, with some dependence in the position of this peak on $\hbar\omega$. Unfortunately, additional characterization of these three factors will be needed before a more quantitative description of the electrode potential dependence can be made. Experimentally, the intensity for pyridine and other neutrals on Ag does show a peak near the point of zero charge [2], with some dependence in the position of these peaks on frequency [22]. However, one also finds that the intensity for different vibrational modes peaks at different potentials [2, 3]. This latter effect would not be contained in the image model predictions unless one could devise a procedure for assigning different R values to different vibrational modes.

IV. Discussion

From these examples we see that the IFE mechanism seems to be capable of predicting a number of different experimental results at least qualitatively. At the same time, however, several groups have criticized certain features of the IFE mechanism [9, 10, 26], and it is appropriate to consider these criticisms here in light of the results of this paper. First,

we note that the IFE mechanism does not require that the surface be rough in order to observe an enhancement. Although no experiments on truly smooth surfaces have been done yet, this statement is not in conflict with the observation of a significant enhancement (10^4) for pyridine on Ag in the absence of cleaning and roughening by electrochemical anodization [3]. However, the IFE theory does not (at first thought) explain the factor of 100 increase in signal associated with anodization, nor does it predict the intense continuous background also observed in many Raman spectra [9, 10]. While it is difficult if not impossible to separate cleaning effects from roughening effects in the anodization process, it is not difficult to show that both will play important roles in the enhancement process even according to the IFE mechanism. Cleaning is important because of the requirement of proximity to the surface in the enhancement process. Even as little as a monolayer of adsorbed material separating the molecule of interest from the metal surface can substantially reduce the enhancement. Proper molecular orientation on the surface can also be influenced by the cleaning process. Roughening, as stated in our original paper on the IFE mechanism [4], can influence the magnitude of the electromagnetic field E_{\sim} on the surface via surface electromagnetic waves [27]. Estimates of the magnitude of the enhancement simply due to this effect have been 10^2 or greater [26b]. This factor would approximately be multiplied by the image field enhancement factor used in Eq. (4) to determine overall enhancement. In addition, any possible frequency and angular dependence in the roughness induced enhancement would be superimposed on the results shown in Figs. 2 and 4, leading to a combination of the effects described by Moskovits [8c] and Pettinger et al. [14a] with the IFE effect. At this point we regard the

continuous background as a separate effect which may very well be due to luminescence from electron-hole pair recombination in the metal as proposed by Burstein et al. [26b]. The absence of interference structure in the Raman spectra at the positions of adsorbate peaks suggests that the background and SERS mechanisms are not coherently coupled, and this agrees with recent time resolved Raman measurements [28], which show very different time scales for the background and molecular scattering.

Another criticism [26c] of the IFE mechanism refers to a paper by Delanaye, Lucas and Mahan [29] which uses an image theory similar but not identical to that described here to calculate shifts in vibrational frequencies which accompany adsorption. The resulting expression for the shifted frequency ω in terms of the "unperturbed" vibrational frequency ω_0 is (for a perfect mirror) $\omega = \omega_0(1 - \alpha_{ZZ}/4R^3)^{1/2}$. If the parameter R is such that $\alpha_{ZZ}/4R^3$ is close to unity (as would be needed to obtain a large image enhancement) the apparent frequency shift will be very large, in gross disagreement with the small (few cm^{-1}) frequency shifts observed experimentally [3]. We would like to point out that the theory of Delanaye, Lucas and Mahan (which has since been modified by the authors [30]) makes an assumption of unknown validity (which is not contained in our theory) concerning the relation between the electronic polarizability α_{ZZ} and certain effective charges which are supposed to represent the adsorbed molecule. Furthermore, this theory has never yielded frequency shifts in agreement with experiment [29, 30] and may even be the wrong mechanism for the frequency shift [31].

One theory which is more closely related to our model (it does not make the above mentioned assumption about effective charges), and which also enables the calculation of frequency shifts is that of Kirtley and Hansma [32]. They avoid representing the molecule by point charges by using a Taylor expansion of the molecular dipole moment about equilibrium. In our notation, their formula for the frequency shift of a harmonic oscillator is (for $\gamma = 1$)

$$\omega = \omega_0 - \frac{(d\mu/dQ)}{8R^3m\omega_0}$$

where $d\mu/dQ$ is the molecular dipole moment derivative, and m the vibrational reduced mass. Taking $d\mu/dQ = 0.5 e$ (a typical value), $R = 1.6 \text{ \AA}$, $m = 10 \text{ AMU}$ and $\omega_0 = 1000 \text{ cm}^{-1}$, we find $\omega - \omega_0 \approx -3 \text{ cm}^{-1}$ which is quite reasonable. While we cannot prove that the Kirtley and Hansma theory is necessarily more accurate than that of Ref. 29 or 30, the present calculation does show that both the SERS enhancement and the frequency shifts can be consistently modelled with what is essentially the same theory.

In concluding this paper we would like to remark that although we have demonstrated many strengths of the IFE approach, certainly extreme caution should be used in making further applications with it, for it is really a very crude approximation to reality and may contain hidden errors which have not yet been revealed.

V. Acknowledgement

We acknowledge support from the Office of Naval Research (Contract N00014-79-C-0794), and the National Science Foundation (Grant CHE-7824866). We also acknowledge helpful discussion with C. Allen and S. Schultz.

References

- [1]a. M. Fleischmann, P. J. Hendra and A. J. McQuillan, *Chem. Phys. Lett.* 26 (1974) 163.
- b. A. J. McQuillan, P. J. Hendra and M. Fleischmann, *J. Electroanal. Chem.* 65 (1975) 933.
- c. R. L. Paul, A. J. McQuillan, P. J. Hendra and M. Fleischmann, *J. Electroanal. Chem.* 66 (1975) 248.
- d. M. Fleischmann, P. J. Hendra, A. J. McQuillan, R. L. Paul and E. S. Reid, *J. Raman. Spectr.* 4 (1976) 269.
- [2]a. D. J. Jeanmaire and R. P. Van Duyne, *J. Electroanal. Chem.* 84 (1977) 1.
- b. R. P. Van Duyne, *J. Phys. (Paris)* 38 (1977) C5.
- [3] R. P. Van Duyne, in: Chemical and Biochemical Applications of Lasers, Vol. 4, Ed. C. B. Moore (Academic Press, New York, 1978), ch. 4.
- [4] F. W. King, R. P. Van Duyne and G. C. Schatz, *J. Chem. Phys.* 69 (1978) 4472.
- [5]a. S. Efrima and H. Metiu, *Chem. Phys. Lett.* 60 (1978) 59.
- b. S. Efrima and H. Metiu, *J. Chem. Phys.* 70 (1979) 1602, 1939, 2297.
- c. S. Efrima and H. Metiu, *Is. J. Chem.*, to be published.
- d. G. L. Eesley and J. R. Smith, preprint.
- [6] F. W. King and G. C. Schatz, *Chem. Phys.* 38 (1979) 245.

- [7] E. Burstein, Y. J. Chen, C. Y. Chen, S. Lundquist and E. Tosatti, Sol. State Comm. 29 (1979) 567; E. Burstein, Y. J. Chen, and S. Lundquist, Bull. Am. Phys. Soc. 23 (1978) 30; R. Fuchs, Bull. Am. Phys. Soc. 24 (1979) 339.
- [8]a. M. R. Philpott, J. Chem. Phys. 62 (1975) 1812.
b. R. M. Hexter and M. G. Albrecht, Spectrochim. Acta 35A (1979) 233.
c. M. Moskovits, J. Chem. Phys. 69 (1978) 4159.
- [9]a. A. Otto, Surf. Sci. 75 (1978) L392.
b. S. L. McCall and P. M. Platzman, Bull. Am. Phys. Soc. 24 (1979) 340.
- [10] J. I. Gersten, R. L. Birke and J. R. Lombardi, Phys. Rev. Lett. 43 (1979) 147.
- [11] J. D. Jackson, Classical Electrodynamics, (John Wiley and Sons, New York, 1962), Chap. 7.
- [12]a. P. B. Johnson and R. W. Christy, Phys. Rev. B6 (1972) 4370.
b. G. B. Irani, T. Huen and F. Wooten, Phys. Rev. B3 (1971) 2385.
- [13] R. G. Greenler and T. L. Slager, Spectrochim. Acta, A29 (1973) 193.
- [14]a. B. Pettinger, U. Wenning and H. Wetzel, preprint;
b. N. V. Richardson and J. K. Sass, Chem. Phys. Lett. 62 (1979) 267.
- [15] C. S. Allen and R. P. Van Duyne, Chem. Phys. Lett. 63 (1979) 455.
- [16] W. C. Meixner and P. R. Antoniewicz, Phys. Rev. B13 (1976) 3276.
- [17] R. R. Smardzewski, R. J. Colton and J. S. Murday, preprint.

- [18] A. P. Lenham and D. M. Treherne, in Optical Properties and Electronic Structure of Metals and Alloys, F. Abeles, Ed., (Wiley, New York, 1966), p. 196.
- [19] V. L. Rideout and S. H. Wemple, *J. Opt. Soc. Am.* 56 (1966) 749.
- [20]a. R. P. Cooney, P. J. Hendra and M. Fleischmann, *J. Raman Spect.* 6 (1977) 264.
- b. M. Fleischmann, P. J. Hendra and A. J. McQuillan, *Chem. Comm.* (1977) 235;
- c. See Also Ref. 1c, but note that the pyridine/Cu spectra reported there cannot be reproduced in our laboratory;
- d. B. H. Loo and T. E. Furtak, to be published.
- [21]a. J. C. Tsang and J. Kirtley, *Solid. State Comm.* 30 (1979) 617;
- b. B. Pettinger, U. Wenning and H. Wetzel, preprint.
- [22] C. S. Allen and R. P. Van Duyne, to be published.
- [23] F. C. Anson, *Acc. Chem. Res.* 8 (1975) 400.
- [24] J. D. E. McIntyre, in Advances in Electrochemistry and Electrochemical Engineering (P. Delahay, C. Tobias, eds.), (Wiley, New York, 1973), p. 61.
- [25] F. Aussenegg, M. Lippitch, R. Moller and Z. Wagner, *Phys. Lett.* 50A (1974) 233.
- [26]a. T. E. Furtak and J. Reyes, preprint.
- b. E. Burstein, C. Y. Chen and S. Lundquist, preprint.
- c. J. Billmann, G. Kovacs, and A. Otto, preprint

- [27] E. Burstein, W. P. Chen, Y. J. Chen and A. Hartstein, *J. Vac. Sci. Tech.* 11 (1974) 1004; Y. J. Chen, W. P. Chen, and E. Burstein, *Phys. Rev. Lett.* 36 (1976) 1207.
- [28] J. Heritage, private communication.
- [29] F. Delanaye, A. A. Lucas and G. D. Mahan, in *Proc. 7th Int. Vacuum Congr. and 3rd Int. Conf. Solid Surfaces*, R. Dobrozemsky et al. (eds.), Vienna, 1977.
- [30] G. D. Mahan and A. A. Lucas, *J. Chem. Phys.* 68 (1978) 1344.
- [31] C. Blyholder, *J. Phys. Chem.* 68 (1964) 2772.
- [32] J. Kirtley and P. K. Hansma, *Phys. Rev. B*, 13 (1976) 2910.

Figure Captions

Fig. 1. Image field model of Raman scattering showing incident beams (1) and (2) of frequency ν , striking the surface at an angle θ_i relative to the normal, and beams (3) and (4) of frequency ν' scattering at an angle θ_o . The dipole μ_{ind} induced in the adsorbed molecule (pyridine) is depicted along with the corresponding image dipole μ_{image} , both at a distance R from the metal-adsorbate interface. The z coordinate of the cartesian system depicted points normal to the surface. Note that the wavelength of light is much larger than R .

Fig. 2. Variation of Raman intensity (in arbitrary units) of s and p polarized scattering light as a function of θ_i or θ_o for Ag at 5490 Å.

Fig. 3 IFE enhancement factor \mathcal{E} as a function of the distance μ_{ind} from the metal surface for Ag at 5214 Å, using $\epsilon_A = 1.76$ and optical constants from Ref. 12. $\sigma = 0.0$ and 0.1 Å results refer to position averaged intensities using Gaussian distributions in R with rms deviation equal to σ .

Fig. 4 Dependence of \mathcal{E} on frequency $\hbar\omega$ (in eV) and λ (in microns) for pyridine on Ag. Theoretical result (solid curve) is for $\epsilon_A = 1.76$, $\sigma = 0.1$ Å and $R = 1.6$ Å. Experimental values are for vibrational frequencies of 1008 cm^{-1} (circles) and 1215 cm^{-1} (squares). Only upper bounds to the experimental results are known in the 3.4-4.0 eV range.

Fig. 5 Dependence of ϵ on frequency for Ag, Au, Cu, and Pt, all for $\epsilon_A = 1.76$, $R = 1.6 \text{ \AA}$. Optical constants are from Refs. 11 (Ag, Au, and Cu), 17 (Pt for $\hbar\omega < 1.6 \text{ eV}$), and 18 (Pt for $\hbar\omega > 1.8 \text{ eV}$). Square denotes estimate of experimental result (Ref. 21b) for Cu at 1.92eV while circle denotes analogous estimate for Au.

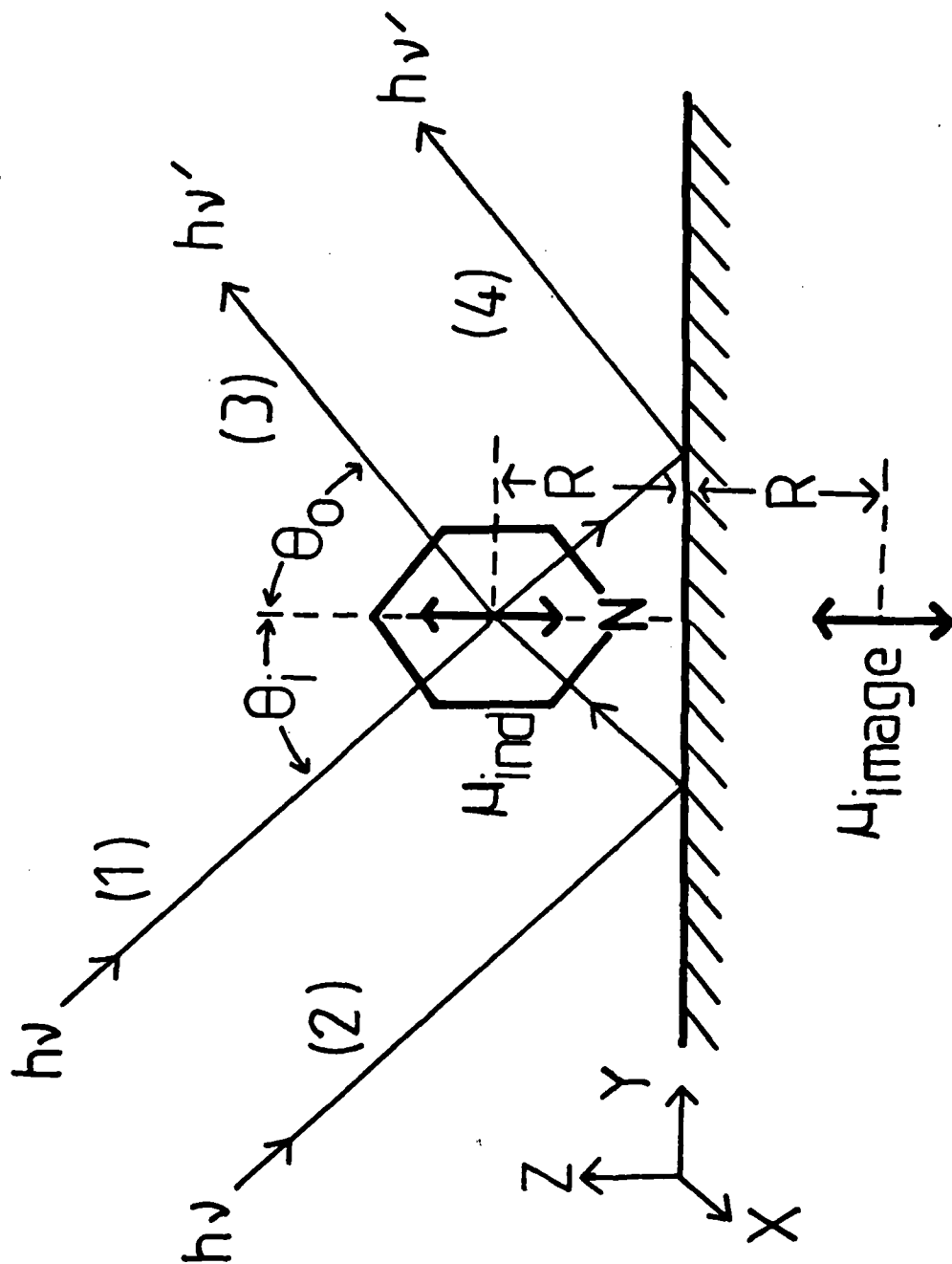


Figure 1

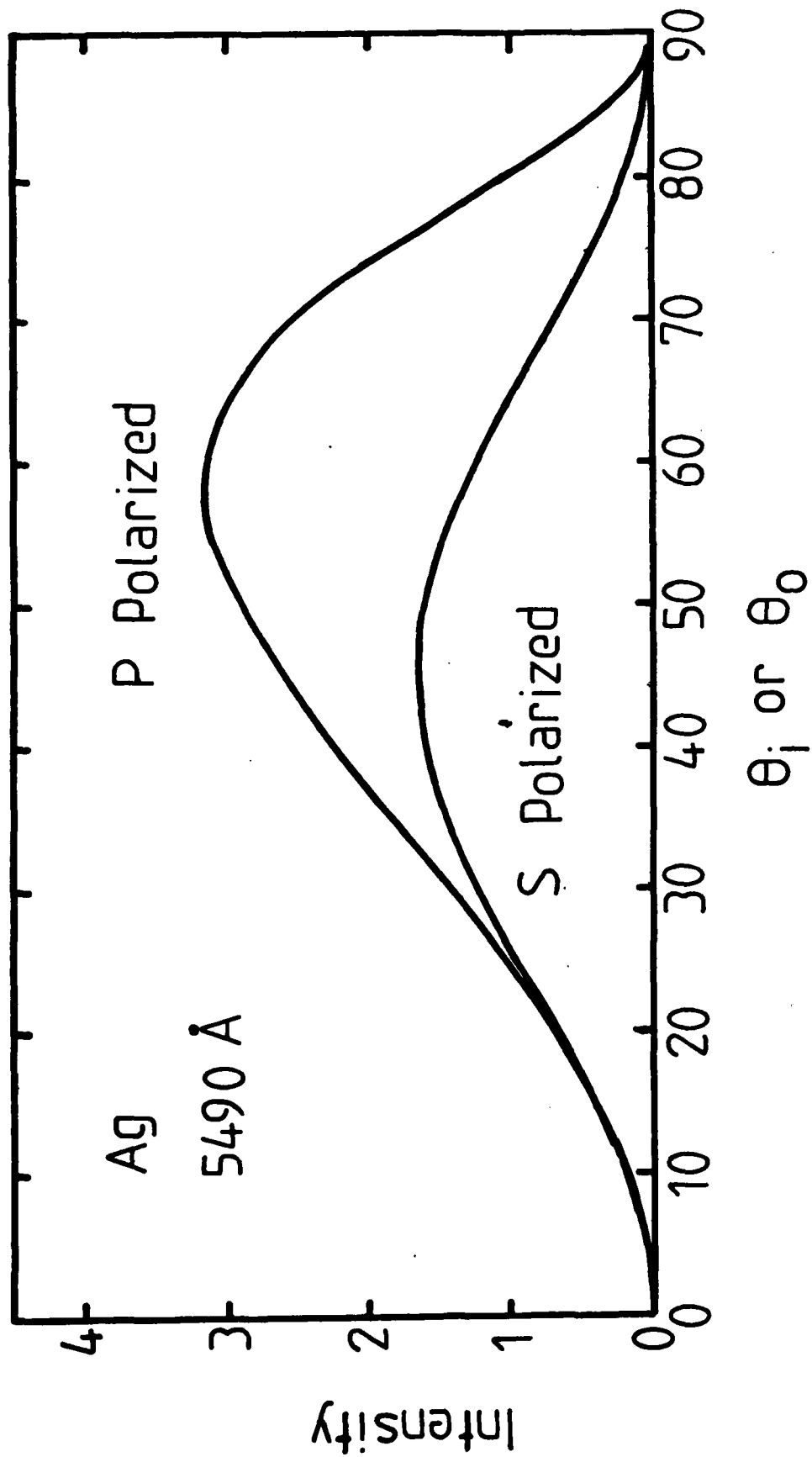


Figure 2

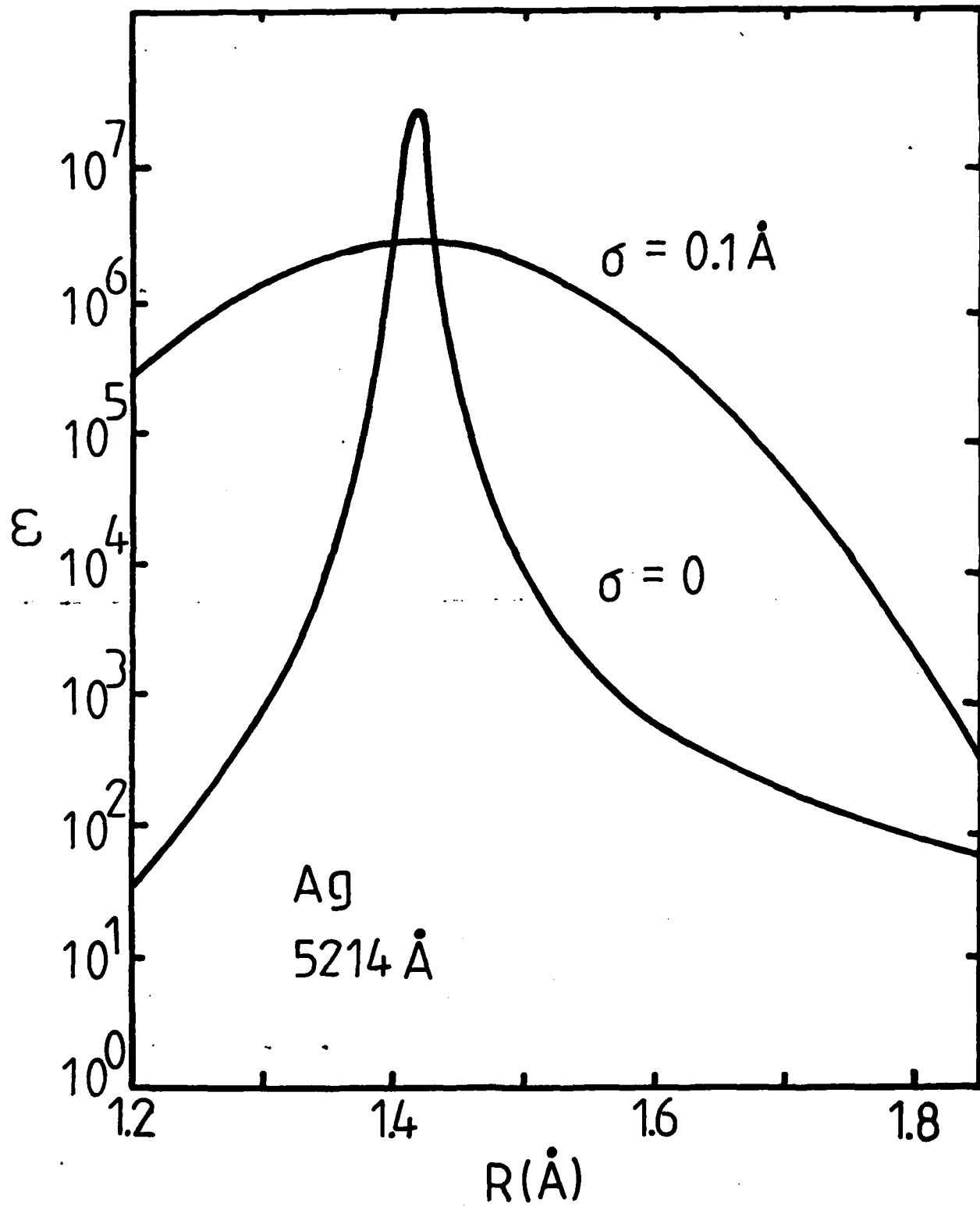


Figure 3

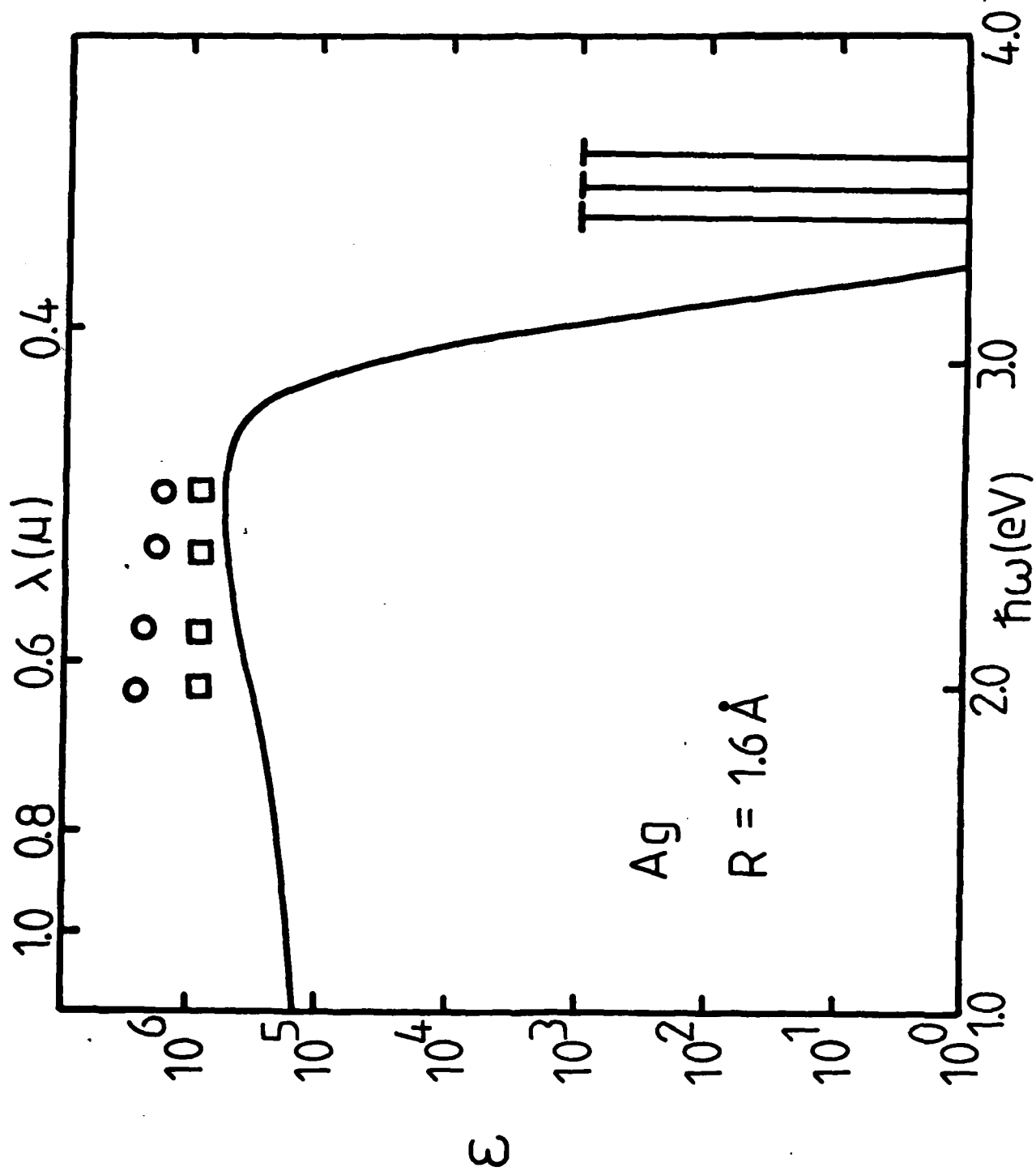


Figure 4

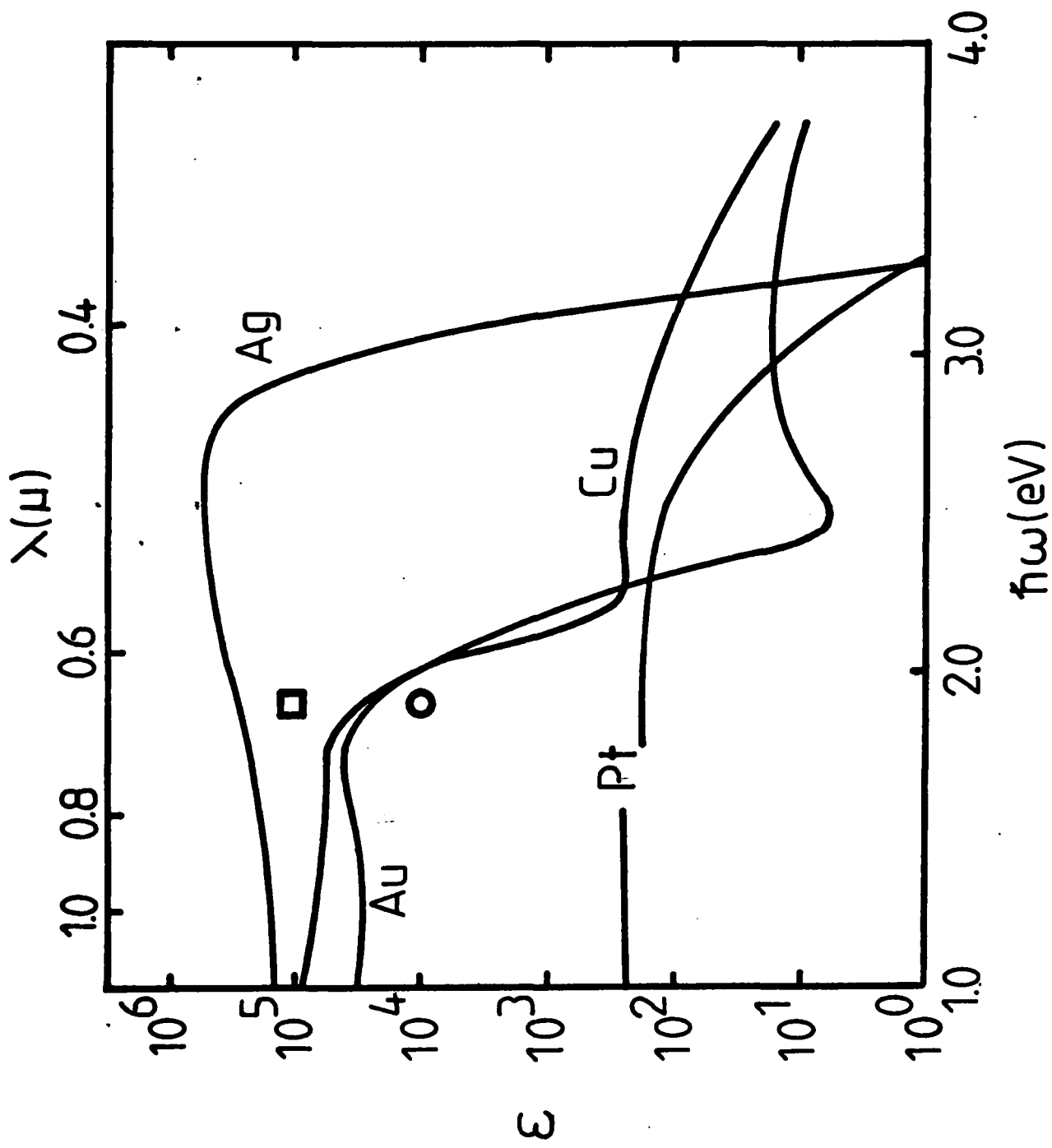


Figure 5